

CALOTROPIS PROCERA EXTRACT (CPE) AS CORROSION INHIBITOR FOR COPPER IN NITRIC ACIDIC MEDIUM

A.S. Fouda¹, A. Abdel Aal², E. Abdel Haleem³

¹Department of Chemistry, Faculty of Science, El-Mansoura University

² Department of Chemistry, Faculty of Science, zagazig University

³ Department of Basic science, Higher Institute of Engineering and Technology in El-Arish

Abstract

The corrosion of copper in 2M HNO₃ in the presence of calotropis procera separate has been researched utilizing, electrochemical impedance spectroscopy (EIS), potentiodynamic polarization (PP), electrochemical frequency modulation (EFM) and weight loss techniques. Polarization studies demonstrated that, this extract acts as mixed- type inhibitor. Inhibition proficiency of this extract has been found to vary with concentration and temperature. The adsorption of this extract on the surface of copper from the corrosive arrangement has been found to obey Temkin adsorption isotherm. The thermodynamic parameters of copper corrosion in 2M HNO₃ were resolved and discussed. The SEM examination and Atomic Force Microscopy (AFM) of the copper surface revealed that the compound prevented from corrosion by adsorption on its surfaces. FTIR results showed that the inhibition mechanism was by absorption process, through the functional groups present in the extract molecules.

Keywords: Calotropis procera extract, Copper corrosion, Inhibitor, HNO₃.

Introduction

An excellent thermal conductivity, good corrosion resistance and mechanical workability are physical properties for copper that explain the wide applications of copper and its alloys in different industries. However, most of the industrial processes lead to corrosion problems. Copper generally corrodes when it is exposed to acids, ammonia, oxygen, or fluids with high sulfur content. Scales and corrosion products have negative influence on heat-transfer, causing a decrease in heating efficiencies of the copper structures [1]. Copper is relatively noble metal, requiring strong oxidants for its corrosion. The chemical dissolution and electro plating are the main processes used in the fabrication of electronic devices. The most widely used nitric acid solution, so



this medium has induced a great deal of research on copper [2-7]. Most well known acid inhibitor is organic compounds containing nitrogen, sulfur, and oxygen atoms. Among them, organic inhibitors have many advantages such as high inhibition efficiency and easy production [8-11]. Organic heterocyclic compounds have been used for the corrosion inhibition of copper [12] in different corroding media. Although many of these compounds have high inhibition efficiencies, several have undesirable side effects, even in very small concentrations, due to their toxicity to humans, deleterious environmental effects, and high cost [13]. Plant extract is low cost and environmental safe, so the main advantages of using plant extracts as corrosion inhibitor are economic and safe environment. Up till now, many plant extracts have been used as effective corrosion inhibitors for copper in acidic media, such as: Zenthoxylum alatum [14], Azadirachta Indica [15], caffeine [16] Cannabis [17]. The inhibition performance of plant extract is normally ascribed to the presence of complex organic species, including tannins, alkaloids and nitrogen bases, carbohydrates and proteins as well as hydrolysis products in their composition. These organic compounds usually contain polar functions with nitrogen, sulfur, or oxygen atoms and have triple or conjugated double bonds with aromatic rings in their molecular structures, which are the major adsorption centers.

The objective of this study was to investigate the inhibitor effect of Calotropis Procera Extract (CPE) as a green corrosion inhibitor for copper in 2M HNO₃ using different techniques. Surface was examined using scanning electron microscopy (SEM) and atomic force microscope (AFM). Fourier Transform Infrared Spectroscopy (FTIR) analysis also used to show the main functional groups of (CPE). The effect of the temperature on the rate of corrosion and thermodynamic parameters were determined and discussed.

Materials and methods

Experimental procedure

Composition of copper samples

Table 1. Chemical composition of the copper, wt %.

Element	Fe	Ni	Si	Pb	Cu
Weight, %	0.0297	0.0103	0.0053	0.023	99.93

Materials and Solutions

Experiments were performed using copper specimens 1cm² as working electrode mounted in Teflon, an epoxy resin was used to fill the space between Teflon and copper electrode. The auxiliary electrode was a platinum

sheet (1cm²), saturated calomel electrode (SCE) as reference electrode was connected to a conventional electrolytic cell of capacity 100 ml via a bridge with a Luggin capillary, the tip of which was very close to the surface of the working electrode to minimize the IR drop. The aggressive solution used was prepared by dilution of analytical grade 70% HNO₃ with bi-distilled water. The stock solution (1000 ppm) of Calotropis Procera was used to prepare the desired concentrations by dilution with bi-distilled water. The concentration range of Calotropis Procera used was 50-300 ppm. The main chemical components of Calotropis Procera are tannins , flavonoids , steroids and saponin glycosides.

Preparation of plant extract

The roots were shade dried at room temperature for 10–15 days and ground into fine powder in a mixer grinder. 200 gram powdered sample was extracted with methanol 70% for 48 hrs . The extract was filtered using Whatman 1 filter paper (pore size 11 μm). The solvent was removed completely under Rotary vaccum. The dried residues were dissolved in 3ml of di methyl sulfoxide (DMSO) and completed to 1000ml with bi-distilled water and finally stored under refrigeration in glass flaske tapered with screw plastic lid.



Figure (1). Calotropis procera plant.

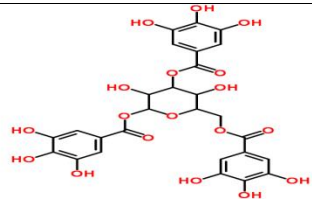
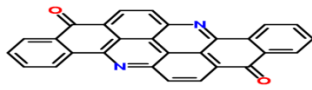
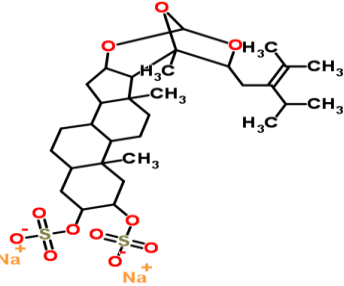
Methods used for corrosion measurements

Weight loss method

The weight loss experiments were carried out using square specimens of size 2 × 2 × 0.5 cm. The specimens were first abraded to a mirror finish using (600, 800 and 1200) grit emery paper, immersed in acetone and finally washed with bi-distilled water and dried before being weighed and immersed into the test solution. The weight loss measurements were carried out in a 100 ml capacity glass beaker placed in water thermostat, which contained 100 ml of 2M HNO₃ with and without addition of different concentrations of

Calotropis Procera Extract (CPE). All the aggressive acid solutions were open to air.

Table 2. Some of the chemical constituents present in calotropis procera extract.

Comp	Structure	IUPAC Name
Tannins		1,3,6-Tris-O-(3,4,5-trihydroxybenzoyl)hexopyranose
Flavonoids (Flavanthrone)		Benzo[5,6]acridino[2,1,9,8-klmna]benzo[h]acridine-8,16-dione
Steroids (Steroid C)		Disodium 22-(2-isopropyl-3-methyl-2-buten-1-yl)-1,3,7-trimethyl-19,21,23trioxahexacyclo[18.2.1.02,18.03,16.06,15.07,12]tricosane-9,10-diyl disulfate

After 3 hours of immersion the specimens were taken out, washed, dried, and weighed accurately. The average weight loss of copper sheets could be obtained. The inhibition efficiency (% IE) and the degree of surface coverage (θ) of Calotropis Procera extract (CPE) for the corrosion of copper was calculated as follows:

$$\% \text{ IE} = \theta \times 100 = [(W^{\circ} - W) / W^{\circ}] \times 100 \quad (1)$$

Where W° and W are the values of the average weight losses in the absence and presence of the inhibitor, respectively. The values of the degree of surface coverage θ were evaluated at different concentrations of the inhibitors in 2M HNO_3 solution.

Potentiodynamic polarization method

Polarization experiments were carried out in a conventional three electrode cell with platinum gauze as the auxiliary electrode (1 cm^2) and a saturated calomel electrode (SCE) coupled to a fine Luggin capillary as reference electrode. The working electrode was in the form of a square cut from copper sheet of equal composition embedded in epoxy resin of poly tetra fluoro

ethylene so that the flat surface area was 1 cm². Prior to each measurement, the electrode surface was pretreated in the same manner as the weight loss experiments. Before measurements, the electrode was immersed in solution at natural potential for 30 min. until a steady state was reached. The potential was started from - 600 to + 400 mV vs. open circuit potential. All experiments were carried out in freshly prepared solutions at 25°C and results were always repeated at least three times to check the reproducibility. % IE and the degree of surface coverage (θ) were calculated from equation (2):

$$\% \text{ IE} = \theta \times 100 = [(i_{\text{corr}} - i_{\text{corr(inh)}}) / i_{\text{corr}}] \times 100 \quad (2)$$

Where i_{corr} and $i_{\text{corr(inh)}}$ are the uninhibited and inhibited corrosion current densities values, respectively.

Electrochemical impedance spectroscopy (EIS) method

Impedance measurements were carried out using AC signals of 5 mV peak to peak amplitude at the open circuit potential in the frequency range of 100 kHz to 0.1 Hz. All impedance data were fitted to appropriate equivalent circuit using the Gamry Echem Analyst software. The experimental impedance were analyzed and interpreted on the basis of the equivalent circuit. The inhibition efficiency (% IE) and the surface coverage (θ) of the investigated inhibitors obtained from the impedance measurements can be calculated from equation (3) [18]:

$$\% \text{ IE} = \theta \times 100 = [1 - (R_{\text{ct}}^{\circ} / R_{\text{ct}})] \times 100 \quad (3)$$

Where R_{ct}° and R_{ct} are the charge transfer resistance in the absence and presence of inhibitor, respectively.

Electrochemical frequency modulation (EFM) technique

EFM experiments were performed with applying potential perturbation signal with amplitude 10 mV with two sine waves of 2 and 5 Hz. The choice for the frequencies of 2 and 5Hz was based on three arguments [19]. The larger peaks were used to calculate the corrosion current density (i_{corr}), the Tafel slopes (β_{c} and β_{a}) and the causality factors CF-2 and CF-3 [20]. All electrochemical experiments were carried out using Gamry instrument.

Surface morphology

The copper surface was prepared by keeping the specimens for three hours in 2M HNO₃ in the presence and absence of optimum concentration of investigated (CPE), after abraded using different emery papers up to 1200 grit size and then polished with Al₂O₃ (0.5m particles size), then washed several times with bi-distilled water and with acetone then immerse it in the solution. After this immersion time, the specimens were washed gently with bi-distilled

water, carefully dried and mounted into the spectrometer without any further treatment. The corroded copper surfaces were examined using an X-ray diffractometer.

FTIR spectra

FTIR spectra were recorded in a Perkin – Elmer 1600 spectrophotometer. The film was carefully removed, mixed thoroughly with KBr made in to pellets and FTIR spectra were recorded.

Atomic Force Microscopy (AFM) Technique

The principle favorable position of AFM is that the roughness of the metal surface can be ascertained which is a measure of the surface of a metal surface. The surface roughness is caused because of deviations of a surface from its optimal shape. AFM examination was completed utilizing Nano Surf Easyscan 2 Flex AFM instruments (Nanotechnology Center, Mansoura University).

Results and discussion

Weight loss tests

Weight loss measurements were carried out for copper in 2M HNO₃ in the absence and presence of different concentrations of CPE are shown in Figure (2). The inhibition efficiency (IE %) values calculated are listed in Table 3. It is noted that the IE% increases steadily with increasing the concentration of the extract and decreases with raising the temperature from 25-45°C which is attributed to physical adsorption. The inhibition efficiency (IE%) and surface coverage(θ) were calculated from equation (1).

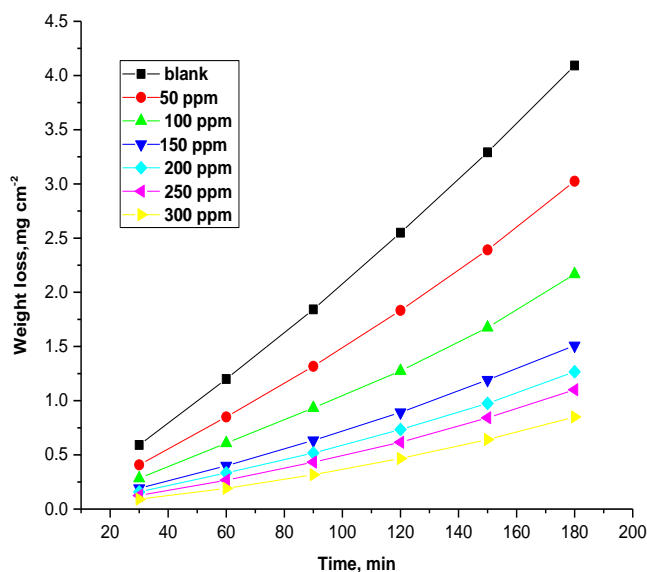


Fig. (2). Weight loss-time curves for the corrosion of copper in 2M HNO₃ in the absence and presence of different concentrations of Calotropis Procera extract at 25°C



Table 3: Corrosion rate (C.R.) and inhibition efficiency data obtained from weight loss measurements for copper in 2M HNO₃ solution without and with various concentrations of CPE at 25°C

Conc., ppm	Weight loss, mg.cm ⁻²	C.R., mg.cm ⁻² .min ⁻¹	Θ	% IE
blank	1.842	0.02
50	1.312	0.015	0.285	28.5
100	0.933	0.01	0.493	49.3
150	0.633	0.007	0.656	65.6
200	0.517	0.006	0.719	71.9
250	0.433	0.0048	0.765	76.5
300	0.317	0.004	0.828	82.8

Table 4: Data of weight loss measurements for copper in 2M HNO₃ solution in the absence and presence of different concentrations of CPE at 25–45 °C.

Conc., ppm	Temp., °C	C.R., Mg/cm ² .min	%IE	Θ
50	25	0.015	28.5	0.285
	30	0.022	25.1	0.251
	35	0.041	19.1	0.191
	40	0.058	15.8	0.158
	45	0.082	9.5	0.095
100	25	0.010	49.3	0.493
	30	0.017	41.4	0.414
	35	0.032	36.3	0.363
	40	0.051	26.5	0.265
	45	0.072	20.4	0.204
150	25	0.007	65.6	0.656
	30	0.011	61.8	0.618
	35	0.024	52.1	0.521
	40	0.037	46.9	0.469
	45	0.053	41.8	0.418
200	25	0.006	71.9	0.719
	30	0.010	66.5	0.665
	35	0.021	58.3	0.583
	40	0.032	53.9	0.539
	45	0.052	42.5	0.425
250	25	0.005	76.5	0.765
	30	0.008	73.7	0.737
	35	0.016	68.3	0.683
	40	0.023	66.4	0.664
	45	0.047	47.6	0.476
300	25	0.004	82.8	0.828
	30	0.006	78.4	0.784
	35	0.012	75.8	0.758
	40	0.022	68.5	0.685
	45	0.030	67.1	0.671

Effect of temperature

The effect of temperature on the corrosion rate of copper in 2M HNO₃ and in presence of different extract concentrations was studied in the temperature range of (25-45) °C using weight loss measurements. As the temperature increases, the rate of corrosion increases, and the inhibition efficiency of the extract decreases as shown in Table 4. The adsorption behavior of extract on copper surface occurs through physical adsorption.

Adsorption isotherms

One of the most convenient ways of expressing adsorption quantitatively is by deriving the adsorption isotherm that characterizes the metal/inhibitor/environment system. Various adsorption isotherms were applied to fit θ values, but the best fit was found to obey Temkin adsorption isotherm which is represented in Figure (3) for Calotropis Procera, Temkin adsorption isotherm may be expressed by:

$$a \Theta = \ln KC \quad (4)$$

Where C is the concentration (ppm) of the inhibitor in the bulk electrolyte, is the degree of surface coverage ($\Theta = \% / 100$), a is heterogeneous factor of surface of metal and K_{ads} is the adsorption equilibrium constant. A plot of Θ versus $\log C$ should give straight lines with slope equal $2.303/a$ and the intercept is $(2.303/a \log K_{ads})$. The variation of the adsorption equilibrium constant (K_{ads}) of the inhibitor with their molar concentrations was calculated according to Eq. (2). The experimental data give good curves fitting for the applied adsorption isotherm as the correlation coefficients (R^2) were in the range (0.943 - 0.999). The equilibrium constant of adsorption K_{ads} obtained from the intercepts of Temkin adsorption isotherm is related to the free energy of adsorption ΔG_{ads}° as follows:

$$K_{ads} = 1/55.5 \exp [-\Delta G_{ads}^{\circ} / RT] \quad (5)$$

Where, 55.5 is the molar concentration of water in the solution in mol/L.

Plots of (ΔG_{ads}°) versus T Figure 4 gave the heat of adsorption (ΔH_{ads}°) and the standard entropy (ΔS_{ads}°) according to the thermodynamic basic equation 6:

$$\Delta G_{ads}^{\circ} = \Delta H_{ads}^{\circ} - T \Delta S_{ads}^{\circ} \quad (6)$$

Table 5 clearly showed a good dependence of ΔG_{ads}° on T, indicating the good correlation among thermodynamic parameters. The negative value of ΔG_{ads}° ensures the spontaneity of the adsorption process and stability of the adsorbed layer on copper surface. Generally, values of ΔG_{ads}° around -20 kJ mol⁻¹ or lower are consistent with the electrostatic interaction between the charged molecules and the charged metal (physical adsorption).

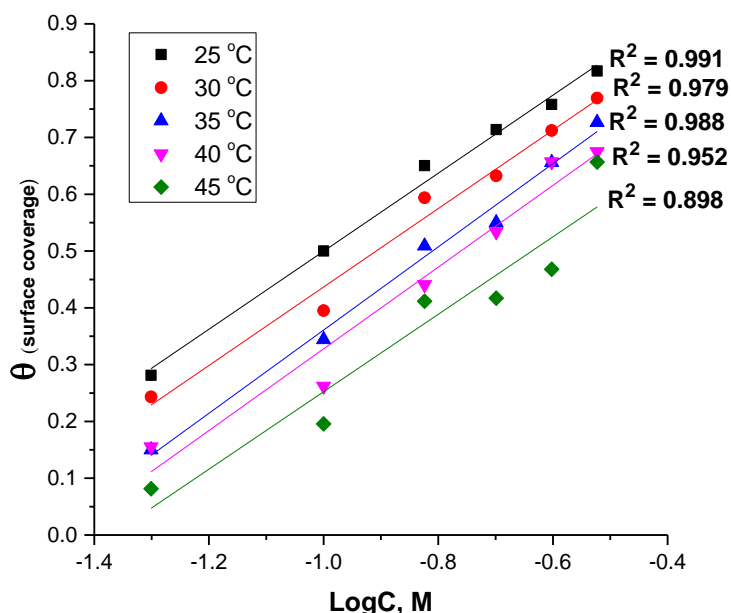


Figure (3). Curve fitting of corrosion data for copper in 2M HNO₃ in presence of different concentrations of Calotropis Procera to the Temkin adsorption isotherm at various temperatures.

The values of thermodynamic parameters for the adsorption of extract (Table 5) can provide valuable information about the mechanism of corrosion inhibition. While an endothermic adsorption process ($\Delta H^{\circ}_{\text{ads}} > 0$) is attributed to an exothermic adsorption process ($\Delta H^{\circ}_{\text{ads}} < 0$) may involve either exothermic adsorption or endothermic adsorption or mixture of both processes. In the presented case, the calculated values of $\Delta H^{\circ}_{\text{ads}}$ for the adsorption of extract in 2M HNO₃ are negative indicating that Calotropis Procera may be physically adsorbed. The $\Delta S^{\circ}_{\text{ads}}$ values are negative which reflects that the inhibitor molecules, freely moving in the bulk solution were adsorbed in an orderly fashion onto the copper surface. This implies that the activation complex in the rate determining step represents an association rather than a, meaning that a decrease in disordering takes place on moving from dissolution step reactants to the activated complex [21].

Table 5: Thermodynamic parameters for the adsorption of Calotropis Procera on copper surface in 2M HNO₃ at different temperatures.

Temp. °K	K _{ads} , M ⁻¹	A	-ΔG ^o _{ads} kJ mol ⁻¹	-ΔH ^o _{ads} kJ mol ⁻¹	-ΔS ^o _{ads} J mol ⁻¹ K ⁻¹
298	1.728	3.35	19.8	32.32	42.18
303	1.632	3.33	19.6		
308	1.493	3.14	19.2		
313	1.456	3.20	19.1		
313	1.37	3.37	19.0		

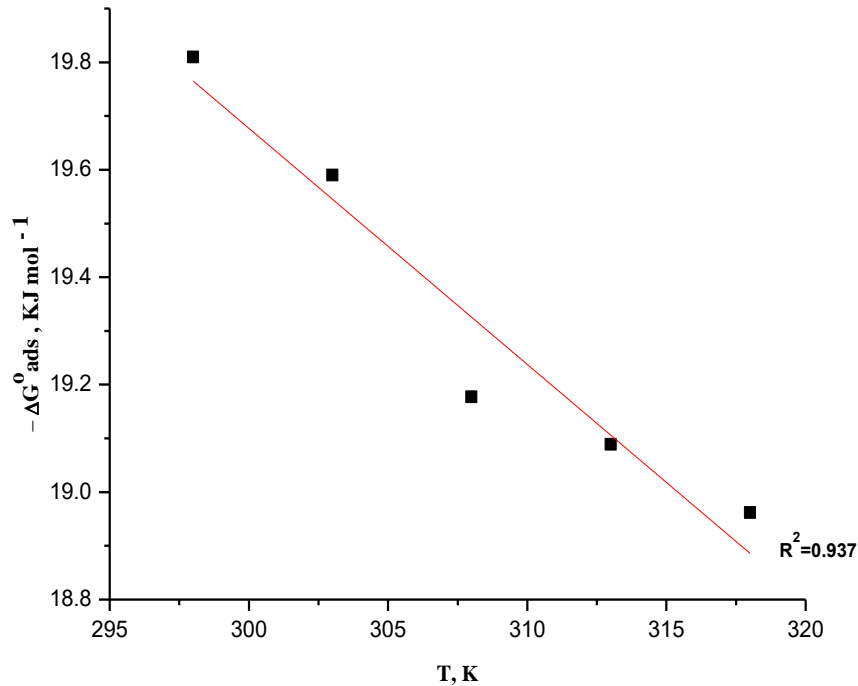


Figure (4). Plots of ΔG°_{ads} vs. T for the adsorption of Calotropis Procera extract on copper in 2M HNO₃

Kinetic Thermodynamic Corrosion Parameters

The activation parameters for the corrosion process were calculated from Arrhenius-type plot according to eq. (7):

$$k_{corr} = A \exp (E_a^* / RT) \quad (7)$$

Where k_{corr} is the rate of metal dissolution, E_a^* is the apparent activation corrosion energy, R is the universal gas constant, T is the absolute temperature and A is the Arrhenius pre-exponential constant. Values of apparent activation energy of corrosion for copper in 2M HNO₃ without and with various concentrations of CPE were determined from the slope of log (k_{corr}) versus 1/T plots and are shown in Figure (5). The alternative formulation of transition state equation is shown in Eq. (8):

$$k_{corr} = (RT/Nh) \exp (\Delta S^*/R) \exp (-\Delta H^*/RT) \quad (8)$$

Where h is Planck's constant, N is Avogadro's number, ΔS^* is the entropy of activation and ΔH^* is the enthalpy of activation. Figure (6) shows a plot of (log k_{corr} / T) against (1/T) in 2M HNO₃. Straight lines are obtained with slopes equal to ($\Delta H^*/2.303R$) and intercepts log ($R/Nh + \Delta S^*/2.303R$), their values are recorded in Table 6. The increase in E_a^* with increase in extract concentration (Table 6) is typical of physical adsorption. The values of ΔH^* reflect the strong adsorption of this extract on copper surface. Moreover, the increase in the activation enthalpy (ΔH^*) in presence of the inhibitor means that the addition of CPE to 2M HNO₃ solution increases the height of the

energy barrier of the corrosion reaction to an extent depends on the concentration of the present extract. The values of entropy (ΔS^*) imply that the activated complex at the rate determining step represents an association rather than a dissociation step, meaning that a decrease in disordering takes place on going from reactants to the activated complex [22,23].

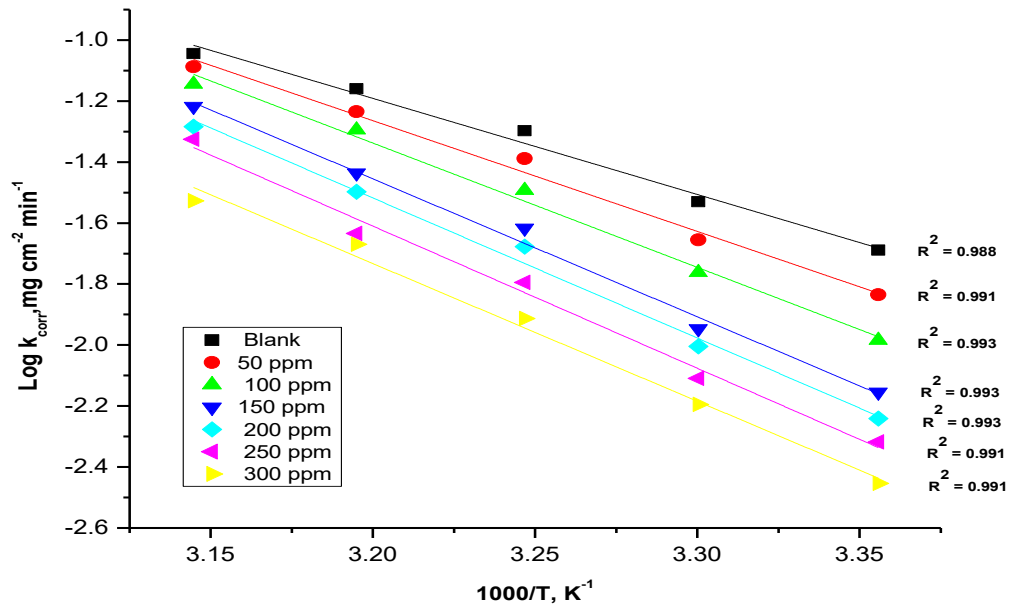


Figure (5). Arrhenius plots of variation of $\log k_{\text{corr}}$ (corrosion rate) vs. $1/T$ for the dissolution of copper in 2M HNO_3 in the absence and presence of different concentrations of CPE

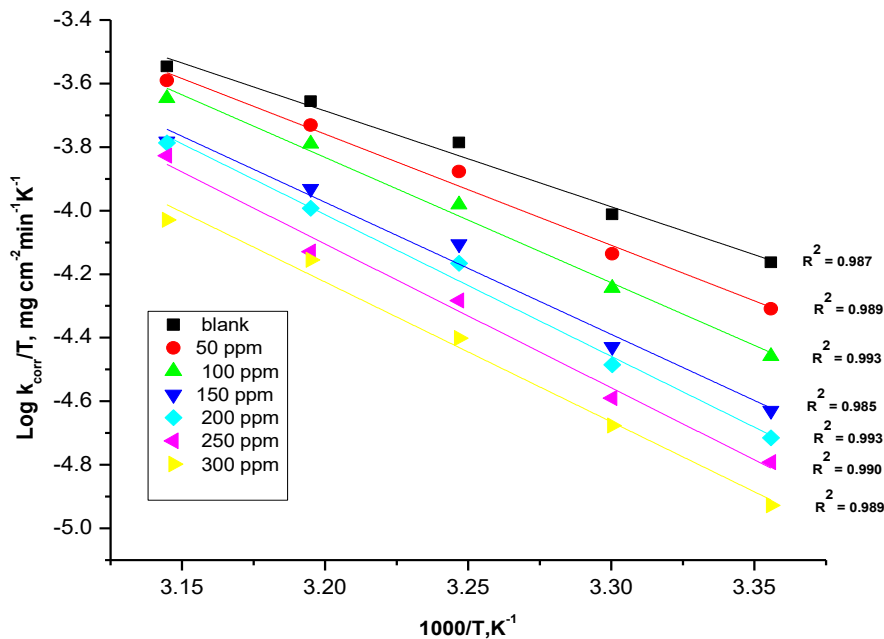


Figure (6). Plots of $(\log k_{\text{corr}} / T)$ vs. $1/T$ for the dissolution of copper in 2M HNO_3 in the absence and presence of different concentrations of CPE

Table 6. Kinetic activation parameters for copper in 2M HNO₃ in the absence and presence of different concentrations of CPE.

Conc., ppm	E _a [*] , kJ mol ⁻¹	ΔH [*] , kJ mol ⁻¹	ΔS [*] - J mol ⁻¹ K ⁻¹
0.0	60	58	83.2
50	70	67	55.2
100	78	75	29.4
150	87	80	18.9
200	88	85	1.2
250	89	87	1.3-
300	92	89	9.0-

Potentiodynamic polarization measurements

Theoretically, copper can hardly be corroded in the deoxygenated acid solutions, as copper cannot displace hydrogen from acid solutions according to the theories of chemical thermodynamics [24]. However, this situation will change in nitric acid. Dissolved oxygen may be reduced on copper surface and this will allow corrosion to occur. It is a good approximation to ignore the hydrogen evolution reaction and only consider oxygen reduction in the nitric acid solutions at potentials near the corrosion potentials [25]. Nitric acid is a strong copper oxidizer capable of rapidly attacking copper. In addition to, the Tafel polarization curves exhibit no steep slope in the anodic range, meaning that no passive films are formed on the copper surface. Polarization measurements were carried out in order to gain knowledge concerning the kinetics of the cathodic and anodic reactions. Figure (7) shows the polarization behavior of copper electrode in 2M HNO₃ in the absence and presence of various concentrations of CPE. The values of electrochemical parameters such as corrosion current densities (i_{corr}), corrosion potential (E_{corr}), cathodic Tafel slope (β_c), anodic Tafel slope (β_a), degree of surface coverage (θ) and inhibition efficiency (% IE) were calculated from the curves of (Figure .7) and are listed in (Table 7) for Calotropis Procera extract.

The results in Table 7 revealed that both the anodic and cathodic reactions are affected by the addition of investigated extract and the inhibition efficiency increases as the extract concentration increases, meaning that the addition of investigated extract reduce the anodic dissolution of copper and also retards the cathodic reactions. In the presence of this extract E_{corr} was enhanced with no definite trend, indicating that this extract act as mixed-type inhibitor in 2M HNO₃, forming an adsorbed layer at the metal/solution interface that decreases the available anodic and cathodic sites.

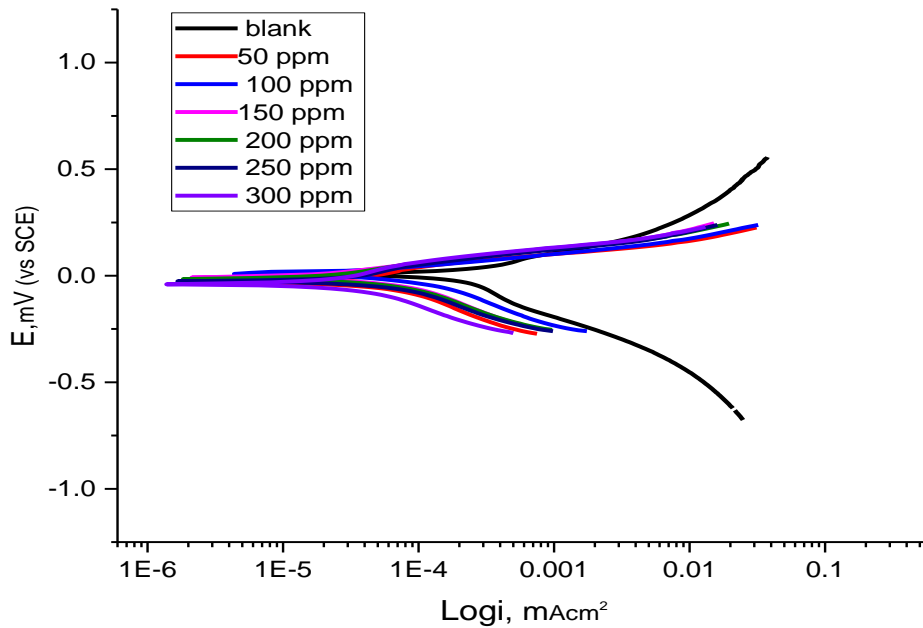


Figure (7). Potentiodynamic polarization curves for the corrosion of copper in 2M HNO₃ in the absence and presence of various concentrations of (CPE) at 25°C

Table 7. Data from potentiodynamic polarization of copper in 2M HNO₃ containing various concentrations of inhibitor at 25 °C.

Conc., ppm	-E _{corr} , mV vs. SCE (vs SCE)	i _{corr} , μA cm ⁻²	β _c mV dec ⁻¹	β _a mV dec ⁻¹	C.R, Mpy	θ	% IE
0	5.8	206	218	138	101.6	----	----
50	29.9	150	443	426	72.72	0.272	27.2
100	24.3	106	294	148	52.38	0.485	48.5
150	25.7	76.3	224	141	37.66	0.629	62.9
200	29.1	50.3	240	150	24.83	0.756	75.6
250	36.5	44.3	351	183	21.84	0.785	78.5
300	40.8	39	274	160	19.26	0.811	81.1

The corrosion current density decreases obviously after the addition of extract in 2M HNO₃ and % IE increases with increasing the extract concentration. % IE and the degree of surface coverage (θ) were calculated from equation (2). As indicated from Table 5, i) the change in β_c values between the extract containing systems and the blank are higher than that of β_a, which indicates that the extract predominantly inhibits cathodic reactions, even though anodic dissolution of copper is also inhibited and ii) The i_{corr} values decrease by the addition of extract. Thus, addition of this inhibitor reduces the copper dissolution as well as, retards the cathodic reaction. Thus, the adsorbed extract acts by simple blocking of the active sites for both anodic and cathodic

processes. Other words, the extract decreased the surface area available for anodic dissolution and oxygen reduction without affecting the reaction mechanism.

Electrochemical Impedance Spectroscopy (EIS) Measurements

Figure (8) shows the Nyquist plots obtained for the copper electrode at respective corrosion potentials after 30 min immersion in 2M HNO₃ in presence and absence of various concentrations of the extract at 25 °C. As the extract concentration increases, the semi-circle diameter increases. The deviation from ideal semicircle was generally attributed to the frequency dispersion as well as to the inhomogenities of the surface [26]. EIS spectra of the investigated extract were analyzed using the equivalent circuit, Figure (9), which represents a single charge transfer reaction and fits well with our experimental results. The constant phase element, CPE, is introduced in the circuit instead of a pure double layer capacitor to give a more accurate fit [27]. The double layer capacitance, C_{dl}, for a circuit including a CPE parameter (Y⁰ and n) were calculated from equation (9) [28]:

$$C_{dl} = Y^0 \omega^{n-1} / \sin [n(\pi/2)] \quad (9)$$

where Y⁰ is the magnitude of the CPE, $\omega = 2\pi f_{max}$, f_{max} is the frequency at which the imaginary component of the impedance is maximal and the factor, n, is an adjustable parameter that usually lies between 0.5 and 1.0. The semi-circle diameter represents the charge transfer resistance, R_{ct}, equivalent to the polarization resistance, R_p, and inversely proportional to the i_{corr} value. An increase in R_{ct} refers to an increase in the thickness of the double layer that adsorbed by inhibitor [29]. In addition, the values of the double-layer capacitance (C_{dl}) decrease by adding inhibitor into corrosive solution. Additionally, double layer capacitance can be calculated with the following equation (10):

$$C_{dl} = \epsilon \epsilon_0 (A/\delta) \quad (10)$$

Where ϵ is the double-layer dielectric constant, ϵ_0 the vacuum electrical permittivity, δ the double-layer thickness, and A is the surface area. Mainly, the decrease in C_{dl} value is attributed to the replacement of the adsorbed water molecules at the metal surface by the extract molecules having lower dielectric constant [30]. Also, the decrease in surface area which acts as a site for charging may be considered as another reason for the C_{dl} decrease [30]. These points suggest that the role of extract molecules is preceded by its adsorption at the metal–solution interface.

The electrochemical parameters were listed in Table (8). The inhibition efficiency was calculated from the charge transfer resistance data from Eq (3).

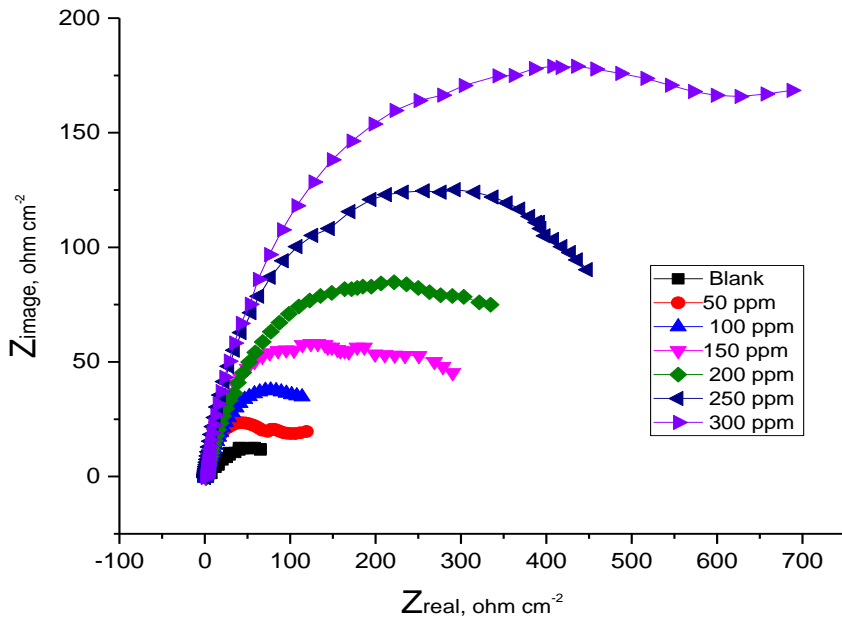


Figure (8). Nyquist plots for copper in 2M HNO₃ in the absence and presence of different concentrations of CPE 25°C.

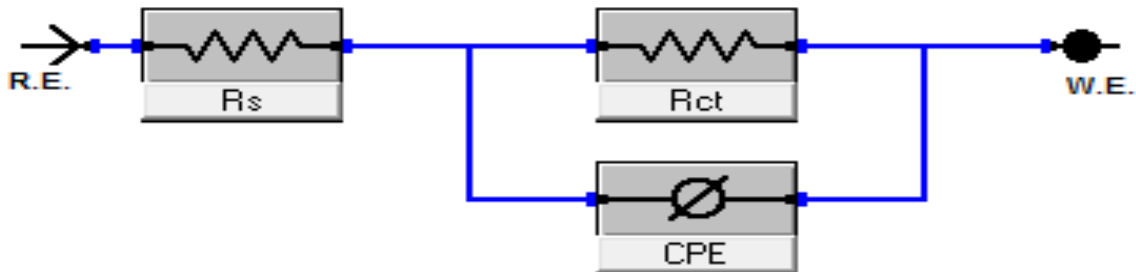


Figure (9). Equivalent circuit used to model impedance data in 2M HNO₃ solutions.

Table 8. Electrochemical kinetic parameters obtained from EIS technique for copper in 2M HNO₃ in the absence and presence of different concentrations of investigated extract at 25°C.

Conc., ppm	N	Y° , $\mu\Omega^{-1}s^n\text{cm}^{-2}$	R_{ct} , Ωcm^2	C_{dl} , μFcm^{-2}	Θ	%IE
0.0	0.768	563.7	97	234	---	---
50	0.728	537.9	123	195	0.207	20.7
100	0.712	432.8	244	174	0.601	60.1
150	0.687	320.9	281	107	0.653	65.3
200	0.632	283.7	365	76	0.733	73.3
250	0.589	242.8	388	47	0.749	74.9
300	0.516	177.9	635	23	0.847	84.7

Electrochemical Frequency Modulation (EFM) Test

EFM is a nondestructive corrosion measurement technique that can directly and quickly determine the corrosion current values without prior knowledge of Tafel slopes, and with only a small polarizing signal. These advantages of EFM technique make it an ideal candidate for online corrosion monitoring [31]. The great strength of the EFM is the causality factors which serve as an internal check on the validity of EFM measurement. The causality factors CF-2 and CF-3 are calculated from the frequency spectrum of the current responses. Figure (10) shows the EFM Intermodulation spectra (current vs frequency) of copper in HNO_3 solution containing different concentrations of CPE.

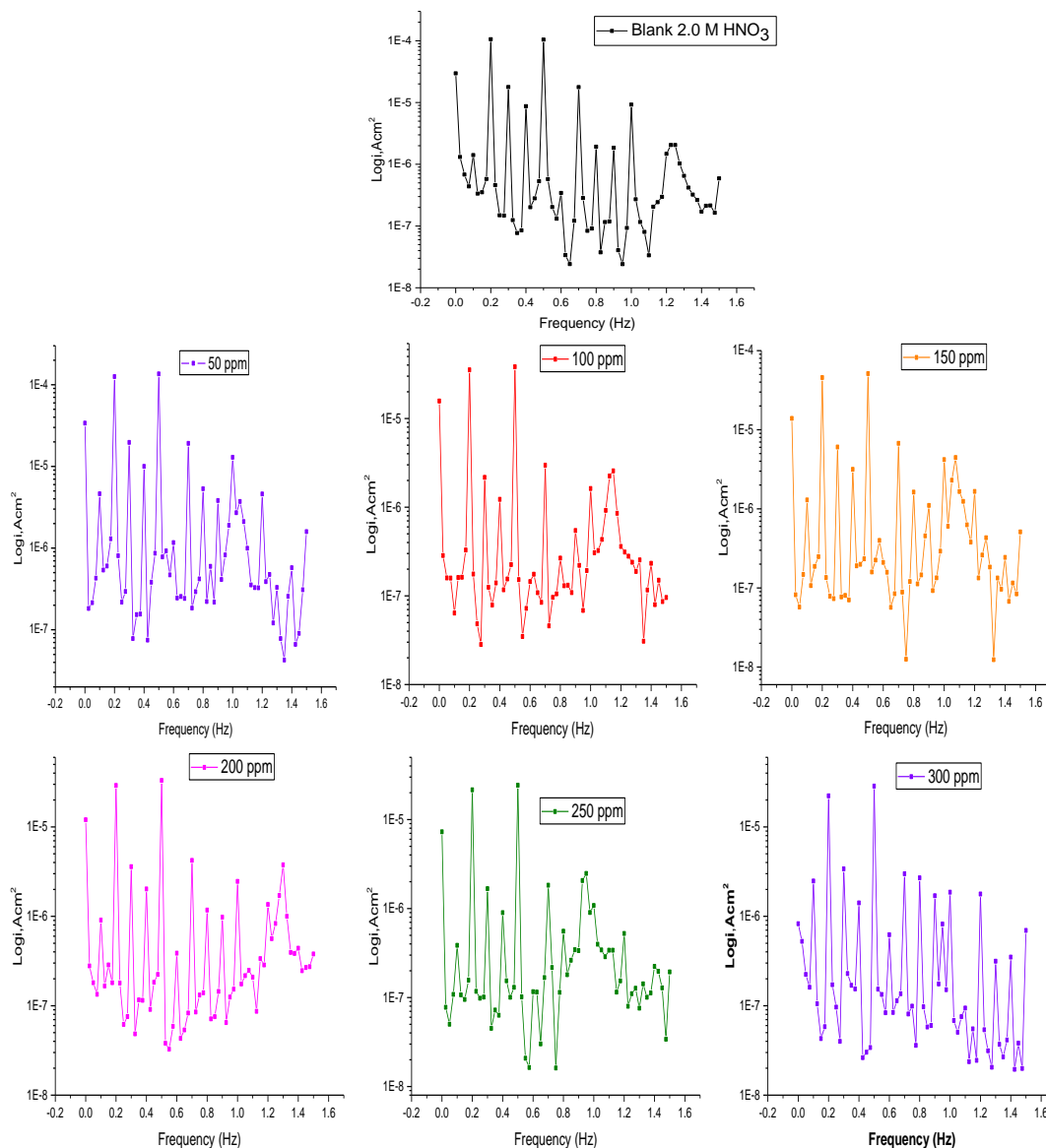


Figure (10). EFM spectra for copper in 2M HNO_3 in the absence and presence of different concentrations of extract at 25°C

The larger peaks were used to calculate the corrosion current density (i_{corr}), the Tafel slopes (β_c and β_a) and the causality factors (CF-2 and CF-3). These electrochemical parameters were listed in Table (9). The data presented in Table (9) obviously show that, the addition of Calotropis Procera at a given concentration to the acidic solution decreases the corrosion current density, indicating that this extract inhibits the corrosion of copper in 2M HNO₃ through adsorption. The causality factors obtained under different experimental conditions are approximately equal to the theoretical values (2 and 3) indicating that the measured data are verified and of good quality. The inhibition efficiencies %IE_{EFM} increase by increasing the inhibitor concentrations and was calculated as from Eq. (2).

Table 9. Electrochemical kinetic parameters obtained from EFM technique for copper in the absence and presence of various concentrations of extract in 2M HNO₃ at 25°C.

Conc., ppm	i_{corr} , μAcm^{-2}	β_c , mVdec^{-1}	β_a , mVdec^{-1}	CF-2	CF-3	C.R, Mpy	Θ	%IE
0.0	260	88	990	1.98	3.57	128.6	-	-
50	141.2	53	103	1.69	3.32	69.68	0.458	45.8
100	80.19	109	204	1.81	2.57	39.57	0.689	68.9
150	56.74	58	110	1.74	3.94	28.0	0.782	78.2
200	32.02	53	90	1.74	2.88	15.8	0.877	87.7
250	30.65	72	109	1.77	2.91	15.13	0.882	88.2
300	16.0	35	49	1.95	3.28	7.74	0.939	93.9

Surface Morphology

In order to verify if the Calotropis Procera molecules are in fact adsorbed on copper surface, scanning electron microscope (SEM) experiments were carried out. The SEM micrographs for copper surface alone and after 24 hrs immersion in 2M HNO₃ without and with the addition of 300 ppm are shown in Figures (11a-c). As expected, (Figure11a) shows metallic surface is clear, while in the absence of CPE, the copper surface is damaged by HNO₃ corrosion (Figure11b). In contrast, in presence of the extract (Figures 11c); the metallic surface seems to be almost no affected by corrosion. The formation of a thin film of CPE observed in SEM micrograph, thus protecting the surface against corrosion.

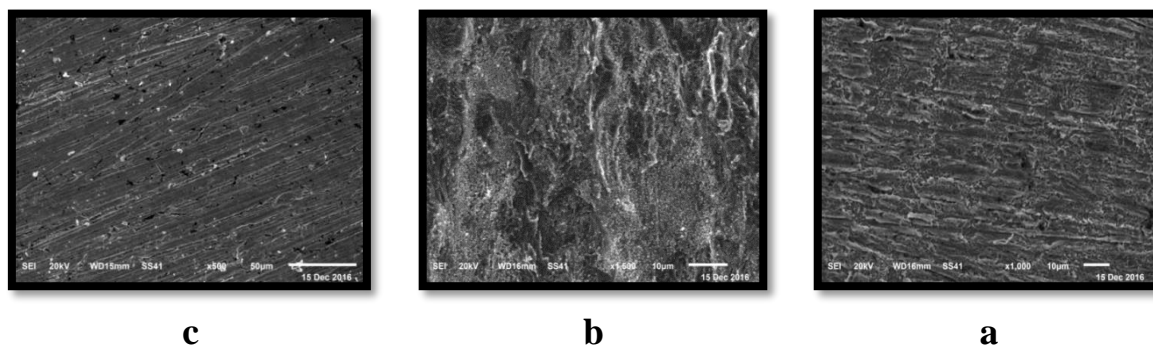


Figure (11): SEM micrographs of copper surface (a) before of immersion in 2 M HNO₃, (b) after 24 hrs of immersion in 2M HNO₃, (c) after 24 hrs of immersion in 2M HNO₃+ 300 ppm Calotropis Procera extract at 25°C.

FTIR Analysis of the Extract and Corrosion Product

FTIR spectroscopy displays interesting features such as high signal to noise ratio, high sensitivity and selectivity, accuracy, mechanical simplicity, short analysis time and small amount of sample required for the analysis [32]. Presented in Fig. (12) show the FTIR spectra of the CPE extract. The broad band obtained at 3390 cm⁻¹ can be assigned to (OH). The frequency at (2970 and 2914) cm⁻¹ corresponds to (C-H) stretching, the one at 1655 cm⁻¹ corresponds to (C=C), the band at 1088 cm⁻¹ can be assigned to (C=S), the sharp one at 1018 cm⁻¹ corresponds to (C-O) stretch and the frequency at 953 cm⁻¹ is due to (=CH₂, =C-H).

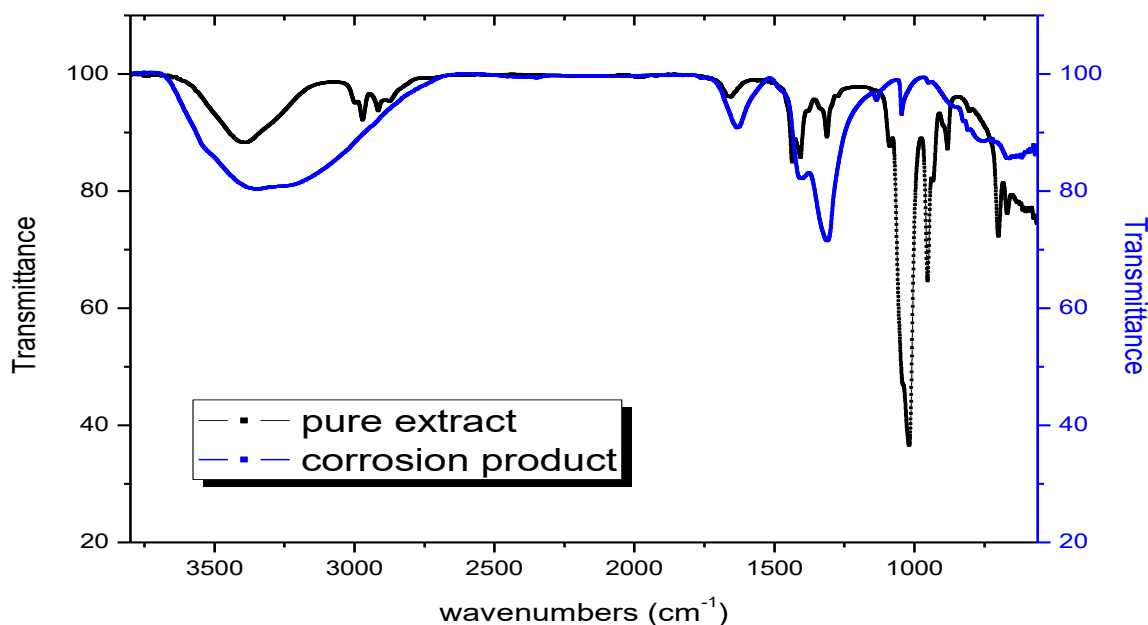


Figure (12). IR spectrum of pure extract and corrosion products of copper after the weight loss test in presence of 300 ppm of the extract at 25 °C.

By comparing the spectra of the calotropis procera extracts with that of the solid corrosion product shown in figure (12), It is observed that there are shifts in the frequencies. It was found that (O-H) stretch at 3390 cm^{-1} was shifted to 3344 cm^{-1} , the C=C stretch at 1655 cm^{-1} was shifted to 1635 cm^{-1} , the (C=S) stretch at 1088 cm^{-1} was shifted to 1135 cm^{-1} , (C-O) stretch at 1018 cm^{-1} was shifted to 1045 cm^{-1} and ($=\text{CH}_2$, =C-H) stretch at 953 cm^{-1} was shifted to 949 cm^{-1} . Indicating that there is interaction between the inhibitor and copper surface. The shifts in the spectra indicate that the interaction between the extract and copper occurred through the functional groups presents in it. Other functional groups were missing suggesting that the adsorption of the inhibitor on the surface of copper might have occurred through the missing bonds [33]. Moreso, it can be affirmed that the functional groups have coordinated with Cu^{2+} formed on the metal resulting in the formation of Cu^{2+} extract complex on the metal surface, which promotes the inhibition of the metal sample.

Atomic Force Microscopy (AFM)

The roughness average values of free metal surface (Fig. 13a), metal in 2M HNO_3 and metal in 2M HNO_3 with Calotropis Procera extract (Fig.13 b, c) were recorded in table 10. The roughness increased in presence of destructive medium (HNO_3) because of the corrosion reaction but in the presence of the Calotropis Procera extract the roughness was decreased due to the adsorption of extract on the copper surface forming defensive layer, demonstrating that the metal surface was became more smoothly and the consumption rate was diminished.

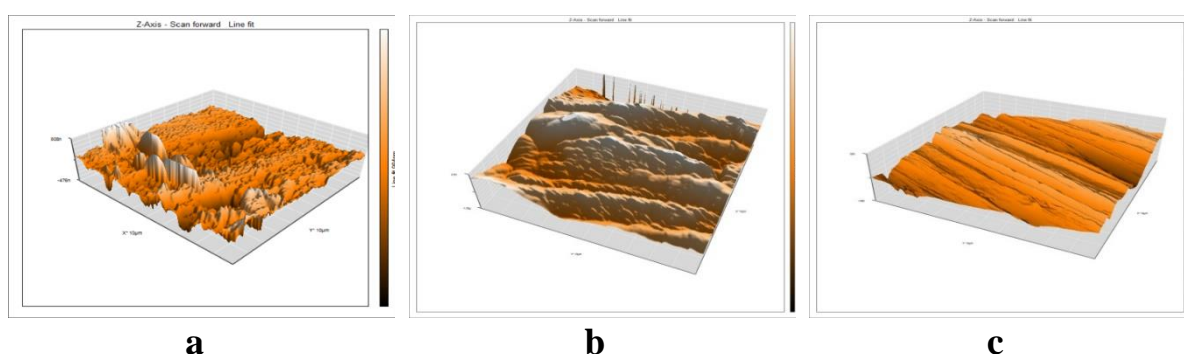


Fig.13: AFM 3D images of for copper (a) free specimen (b) with 2M HNO_3 for 4 hrs (c) with 2M HNO_3 containing 300 ppm Calotropis Procera extract for 4 hrs.



Table 10: AFM parameters for copper (a) free specimen (b)with 2M HNO₃ for 4 hrs (c) with 2M HNO₃ containing 300 ppm Calotropis Procera extract for 4 hrs.

Parameters	A	B	C
The roughness average (Sa)	24.9	163.1	104.4
The mean value (Sm)	-18.9	-18.5	-15.1
The root mean square (Sq)	31.6	203.1	139.5
The valley depth (Sv)	-88.6	1050.6-	-604.1
The peak height (Sp)	81.5	598.6	932.9
The peak valley height (Sy)	170.1	1649.2	1537.1

Inhibition mechanism

In acidic solutions, transition of the metal/solution interface is attributed to the adsorption of the inhibitor molecules at the metal/solution interface, forming a protective film. The rate of adsorption is usually rapid, and hence, the reactive metal surface is shielded from the acid solutions. Inhibition of the copper corrosion in 2M HNO₃ by the investigated extract as indicated by weight loss, potentiodynamic polarization, electrochemical impedance spectroscopy, electrochemical frequency modulation and other methods were found to depend on the number of adsorption sites in the molecules that present in CPE extract and their charge densities, molecular size and stability of these additives in acidic solution. The observed corrosion data in presence of this inhibitor, namely:

- i) The decrease of corrosion rate and corrosion current with increase in concentration of the inhibitor.
- ii) The linear variation of weight loss with time.
- iii) The shift in Tafel lines to higher potential regions.
- iv) The decrease in corrosion inhibition with increasing temperature indicates that desorption of the adsorbed inhibitor molecules takes place.
- v) The inhibition efficiency was shown to depend on the number of adsorption active centers in the molecules and their charge densities.

The corrosion inhibition is due to adsorption of the extract at the electrode/solution interface, the extent of adsorption of the extract depends on the nature of the metal, the mode of adsorption of the extract and the surface conditions. Adsorption on copper surface is assumed to take place mainly through the active centers attached to the extract and would depend on their charge density. It was concluded that the mode of adsorption depends on the affinity of the metal towards the π -electron clouds of the ring system. Metals such as copper, which have a greater affinity towards aromatic moieties, were found to adsorb benzene rings in a flat orientation and the functional groups

have coordinated with Cu^{2+} formed on the metal resulting in the formation of Cu^{2+} extract complex on the metal surface, which promotes the inhibition of the copper sample.

Conclusions

Based on the above results of this study, the following conclusions can be drawn:

1. The studied plant extract (CPE) is effective inhibitor for corrosion of copper exposed to 2M HNO_3 solution.
2. The adsorption of extract depends on its concentration, degree of temperatures and the nature of the inhibitor and metal.
3. Reasonably good agreement was observed between the values obtained by the weight loss and electrochemical measurements.
4. Results obtained from potentiodynamic polarization indicated that CPE is mixed-type inhibitor.
5. Percentage inhibition efficiency of *Calotropis Procera* was temperature dependent and its addition led to an increase of the activation corrosion energy.
6. The adsorption of *Calotropis Procera* onto copper surface follows the Temkin adsorption isotherm model.
7. Thermodynamic parameters revealed that the inhibition of corrosion by *Calotropis Procera* extract is due to the formation of a physical adsorbed film on the metal surface.
8. The SEM and AFM images of the copper samples showed that the metal was protected in the presence of the extract.
9. FTIR analysis of the extract and corrosion product showed the functional groups that have coordinated with Cu^{2+} .

References

- F.K. Crundwell, The anodic dissolution of copper in hydrochloric acid solutions, *Electrochim. Acta* 37, (1992),2101
- K.Barouni, M.Mihit, L.Bazzi, R.Salghi, S.S. Al-Deyab, B.Hammouti, A.Albourine, The Inhibited Effect of Cysteine Towards the Corrosion of Copper in Nitric Acid Solution, *The open corrosion j.*, 3, (2011) ,58
- Zarrouk, B. Hammouti, H. Zarrok, M. Bouachrine, K.F. Khaled, S.S. Al-Detab. Corrosion inhibition of copper in nitric acid solutions using a new triazole derivative. *J.Electrochem.sci.*,7, (2012),89
- B.V.Appa Rao, Md. Yakub Iqbal, B.Sreedhar, Electrochemical and surface analytical studies of the self assembled monolayer of 5-methoxy-2-



- (octadecylthio) benzimidazole in corrosion protection of copper
Electrochimica Acta, 55,(2010),620-631
- A.Fiala, A.Chibani, A.Darchan, A.Boulkamh, K.Djebbar, Investigations of the inhibition of copper corrosion in nitric acid solutions by ketene dithioacetal derivatives *Appl.Surf.Sci.*,253,(2007),9347
- K.F.Khaled, Corrosion control of copper in nitric acid solutions using some amino acids A combined experimental and theoretical study *Corrosion sci.*, 52, (2010) , 3225
- K.F.Khaled, Sahar A. Fadl-Allah, B.Hammouti, Some benzotriazole derivatives as corrosion inhibitors for copper in acidic medium: Experimental and quantum chemical molecular dynamics approach *Materials-Chemistry-and-Physics*,117,(2009),148
- D. N. Singh and A. K. Dey. Inhibition effect of nonionic surfactant on the corrosion of cold rolled steel in hydrochloric acid. *Corrosion. Sci.* 49, (1993),594
- G.Banerjee and S. N. Malhotra. Contribution to Adsorption of Aromatic Amines on Mild Steel Surface from HCl Solutions by Impedance, UV, and Raman Spectroscopy *Corrosion. Sci.* 48, (1992),10
- S.T Arab and E.A.Noor. Inhibition of Acid Corrosion of Steel by Some S-Alkylisothiuronium Iodides *Corrosion. Sci.* 49,(1993),122
- I.A.Raspini. Influence-of-Sodium-Salts-of-Organic-Acids-as-Localized-Corrosion-of-Aluminum-and-Its-Alloys. *Corrosion.Sci.* 49,(1993),821
- R.F.Villamil, P.Corio and J.C.Rubim. Inhibition of copper corrosion by 1,2,3-benzotriazole. *J. Electroanal. Chem.* 472, (1999),112
- K.S.karikh, K.J.Joshi, K.S.Parikh Natural products as corrosion inhibitor for metals in corrosive media, *Trans. SAEST*, 39,(2004),29
- J.S.Chauhan .Anticorrosion Behaviour of Zenthoxylum alatum Extract in Acidic Media, *Asian J. of Chemistry.* 21, (2009),1975
- T.V.Sangeetha ,M.Fredimoses .Inhibition of Mild Copper Metal Corrosion in HNO₃ Medium by Acid Extract of Azadirachta Indica Seed, *E-J. of Chemistry*, 8,(2011),S1-S6
- F. S. Souza, C. Giacomelli and R. S. Gonçalves. Corrosion Inhibition of Carapichea Ipecacuanha Extract (CIE) on Copper in 1M HNO₃ Solution, *Materials Science and Engineering.* 32, (2012),2436
- B.A.Abd-El-Nabey, A. M. Abdel-Gaber, M. A. El. Said, E. Khamis and S. El-Housseiny . Inhibitive Action of Cannabis Plant Extract on the Corrosion of Copper in 0.5 M H₂SO₄, *J. Electrochem. Sci.* 8, (2013), 5851
- H .Ma, S.Chen, , L .Niu, , S. Zhao, , S. Li, , D. Li, Inhibition of copper corrosion by several Schiff bases in aerated halide solutions, *J. of Applied Electrochemistry*,32,(2002),65



- R. W. Bosch, J. Hubrecht, W. F. Bogaerts, B. C. Syrett, Electrochemical Frequency Modulation: A new Electrochemical Technique for Online Corrosion Monitoring. *Corrosion* 57, (2001), 60
- S. S. Abdel-Rehim, K. F. Khaled, N. S. Abd-Elshafi, Electrochemical frequency modulation as a new technique for monitoring corrosion inhibition of iron in acid media by new thiourea derivative, *Electrochim. Acta* 51, (2006), 3269
- G. Banerjee, S. N. Malhotra, Contribution to Adsorption of Aromatic Amines on Mild Steel Surface from HCl Solutions by Impedance, UV, and Raman Spectroscopy, *Corrosion*. 48, (1992), 10
- Hour. T. P. & Holliday. R. D., Trigoneella stellate extract as corrosion inhibitor for copper in 1M nitric acid solution, *J. of Metallurgy*. 3, (1953), 502
- L. O. Riggs, Jr., T. J. Hurd, Trigoneella stellate extract as corrosion inhibitor for copper in 1M nitric acid solution, *Corrosion*, 23, (1967), 252
- A. Muller, W. Stockel, Schumacher, A study on the mechanism of the electrochemical dissolution of copper in oxygenated sulphuric acid: An application on the quartz microbalance, *J. Electroanal. Chem.*, 219, (1987) 311
- W. H. Smyrl, J. O. M. Bockris, B. E. Conway, E. Yeager, R. E. White (Eds.), *Comprehensive Treatise of Electrochemistry*, Intenum Press, New York, 4, (1981), 116.
- M. El Achouri, S. Kertit, H. M. Gouttaya, B. Nciri, Y. Bensouda, L. Pere M. R. Infante, K. Elkacemi, Corrosion inhibition of iron in 1M HCl by some Gemini surfactants in the series of alkanediyl α, ω bis-(dimethyl tetradecyl ammonium bromide), *Progress in Organic Coatings*, 43, (2001), 267
- J. R. Macdonald, W. B. Johanson, J. R. Macdonald (Ed.), *John, Wiley & Sons, Interaction of cysteined copper ions on the surface of iron: EIS, polarization and XPS study*, book chapter 1, New York, (1987), 1
- S. F. Mertens, C. Xhoffer, B. C. Decooman, E. Temmerman, Short Term Deterioration of Polymer Coated 55% Al Zn Part 1: Behavior of Thin Polymer Films. *Corrosion* 53, (1997), 381
- M. Lagrenée, B. Mernari, M. Bouanis, M. Traisne, and F. Bentis Study of the mechanism-and-inhibiting efficiency of 3,5 bis(4-methylthiophenyl) 4H 1,2,4 triazole on mild steel corrosion in acidic media, *Corrosion Science*, 44, (2002), 573
- F. Bentiss, M. Lagrenée, and M. Traisnel, 2,5 Bis(n-Pyridyl) 1,3,4 Oxadiazoles as Corrosion Inhibitors for Mild Steel in Acidic Media, *Corrosion*, 56, (2000), 733
- F. M. Reis, H. G. Melo, I. Costa, EIS investigation on Al 5052 alloy surface preparation for self assembling monolayer, *Electrochim. Acta*. 51, (2006), 17



- Hortling, B., Tamminen, T. & Kentta, E. Determination of Carboxyl and Non Conjugated Carbonyl Groups in Dissolved and Residual Lignins by IR Spectroscopy, *Holzforschung*, 51, (1997), 405
- Ebenso E.E., Eddy N.O., Odiongenyi A.O., Afri. J. Corrosion inhibitive properties and adsorption behaviour of ethanol extract of *Piper guinensis* as a green corrosion inhibitor for mild steel in H_2SO_4 , pure and *Appl. Chem.*, 4, (2008), 107

الملخص العربي

يتضمن هذا البحث استخدام طريقه الفقد في الوزن لمعرفة تأثير درجة الحرارة على تثبيط تآكل النحاس في محلول حمض النيتريك في مدى درجات الحرارة 25-45 درجة مئوية، و وجد أن معدل التآكل يزداد بزيادة درجة الحرارة مع نقص كفاءة التثبيط في حاله مستخلص العشار الثاقب و يتبع ايزوثرم تمكن وذلك بعد رسم علاقة بين θ و $\log C$, امكن الحصول علي الدوال ΔG°_{ads} , ΔH°_{ads} , ΔS°_{ads} ومن خلال قيم ΔG°_{ads} تبين أن التثبيط يحدث عن طريق ادمصاص فيزيائي. وحيث ان القيم السالبة لل ΔG° تبين ان عمليه الامتزاز على سطح النحاس تتم تلقائيا.

يتضمن البحث ايضا دراسة تأثير مستخلص العشار الثاقب على الاستقطاب المهبطي و المصعدي النحاس في محلول حمض النيتريك و وجد أن هناك إزاحة لمنحنيات الاستقطاب المهبطي و المصعدي على السواء و بتطبيق معادلة تافل وجد أن معدل التآكل يقل مع زيادة التركيز للمثبط و بالتالي زيادة كفاءة عملية التثبيط مع استخدام نفس التركيزات المستعملة في حالة (طريقة فقد الوزن).

كما جاءت النتائج المستخرجة باستخدام تقنية المعاوقة الكهروكيميائية الطيفية أن عملية تآكل النحاس في محلول حمض النيتريك في عدم وجود ووجود هذا المستخلص محكومة بانتقال الشحنة وأن زيادة تركيز المثبطات تؤدي إلى زيادة قيم مقاومة انتقال الشحنات (R_{ct}) مقابل تدنى قيم الطبقة المزوجة (C_{dl}).

وايضا جاءت نتائج القياسات لقيم تيار التآكل (i_{corr}) بواسطة تقنية " التردد الكهروكيميائي المعدل (EFM) متوافقه مع قيم تيار التآكل (i_{corr}) الناتجة من خلال طريقة الاستقطاب.

كما أظهر تحليل مسح المجهر الإلكتروني أن تثبيط مستخلص العشار الثاقب تمت من خلال امتزاز هذا المستخلص على السطح المعدني الذي يشكل طبقة رقيقة يحمي المعدن من التآكل.

وايضا اظهر تحليل طيف الاشعه تحت حمراء وجود مجموعات وظيفيه فعاله في تركيب المستخلص النباتي وانها تتفاعل مع سطح النحاس مكونه مركبات مع النحاس على سطحه تعمل على تكوين طبقة حمايه لسطح النحاس من التاكل في حامض النيتريك.

كما اوضح تحليل مجهر القوة الذرية انخفاض نسبه خشونه السطح في حاله وجود المستخلص وبالتالي تتكون طبقات حمايه لسطح النحاس من التاكل وبالتالي يصبح السطح اكثر نعومه وينخفض معدل الاستهلاك والتآكل.